Performance and Emission Characteristics of Diesel-Biodiesel-Ethanol Blends in a Heavy-Duty Compression Ignition Engine at Simulated High Altitudes

Julio C. Cuisano and Solin E. Puma
Mechanical Department of Engineering Faculty
Pontificia Universidad Católica del Perú
Lima, Perú
jcuisano@pucp.edu.pe, spuma@pucp.edu.pe

Abstract

The effects of anhydrous ethanol (E) and castor oil (R) mixed with diesel fuel (D), commercially containing 5% biodiesel by volume, were researched experimentally to evaluate the combustion process and specific fuel consumption in a compression ignition engine, supercharged, six cylinders. In total, three mixtures were used, varying the diesel content from 95% (D95) to 80% v/v (D85), obtaining the following compositions: D95B0E0, D85B6E9 and D80B6.5E13.5. The experimental tests were performed in stationary conditions (1000 and 1800 rpm), two values of effective torque (80, and 160N.m) and two conditions of intake air pressure (100 and 80 kPa). The results obtained show that the mixtures containing ethanol and biodiesel lead to an early start of combustion at 1000 rpm and a delay at the start of combustion at 1800 rpm. The increase in ethanol and biodiesel over commercial fuel does not have any influence on specific fuel consumption; however, the altitude effect generates an increase in specific fuel consumption up to 11% and 7% at 1000 rpm and 1800 rpm respectively. The specific emissions of NO_X, CO and $CO_2$are increased with higher specific fuel consumption; in addition, the effect of simulated altitude allowed to verify that at higher altitudes there is a slight increase in sfc and EE of CO and CO_2, together with a reduction in EE NO_X. At 2000 m of simulated altitude (APCI = 80 kPa) the maximum increases of sfc, CO and CO_2, with the mixture D80B6.5E13.5, were 5%, 122% and 18%, respectively. And the maximum reductions in NO_X EE were also obtained with the D80B6.5E13.5 mixture, reaching decreases of up to 6%.

Keywords
Diesel, ethanol, Combustion, Specific fuel consumption, Emissions

1. Introduction

Alternative internal combustion engines have developed a very important role in the industrial development of society. Compression ignition engines (MEC) have better thermal efficiency compared to positive ignition engines (MECH); However, due to the higher compression ratio of MECs and the use of poor air-fuel mixtures, these are the cause of high emissions of nitrogen oxides, NO_X and particulate matter, PM (Heywood, 2018). And as the altitude where these engines operate increases, there is a drop in thermal performance and they use emissions of carbon monoxide, CO, hydrocarbons, HC and PM (He et al., 2011).

Regarding diesel fuel, the Organization of the Petroleum Exporting Countries (OPEC) affirms that the world demand will grow faster than any other distilled product, towards the year 2030 (OPEC, 2019). Likewise, it is indicated that biofuels will have a greater demand as they form a volumetric part instead of diesel; A common blend of diesel with biodiesel and gasoline with ethanol is B20 and E10, 20% biodiesel replacing diesel and 10% ethanol replacing gasoline, respectively, in the US (Eia, 2018).

In Peru, as in other Latin American countries, the fuel with the highest demand is diesel, representing, on average, 53% of the fuel market since 2013, due to its great use in transportation, residential and other sectors. commerce, industries, mining, public, agriculture and fishing (GPAE, 2017). And due to the low quality of fuels, in Peru, since 2018, the Euro IV, Tier 2 and EPA 2007 vehicle emission standards have been in force (MINAM, 2018).
Furthermore, by national law, commercialized diesel and gasoline must not contain sulfur in a concentration higher than 50 ppm. In addition, diesel contains 5% biodiesel and gasoline 7.8%, by volume. But there is no projection of an

increase in the percentage of these biofuels mixed with diesel and gasoline due to a political initiative (USDA, 2018). To comply with this percentage of biodiesel, since 2012, the country has been importing 95% of its internal consumption; And in the case of ethanol, since 2017, it went from exporter to importer, due to various commercial factors that led to the production of sugar instead of biofuel. In the last two years, national ethanol production represented, on average, 87% of its domestic consumption (USDA, 2018).

Peru has potential agricultural areas for the production of biodiesel and bioethanol (USDA, 2018). The application of fiscal incentives for the production of biofuels, and a greater number of studies on the use of ethanol in engines that operate at different altitude conditions, typical of countries influenced by the Andes Mountains, would contribute to reducing the impact of the balance. . trade deficit in the fuel sector in Peru and in other countries of the high Andean region. Peru, being a country with a millenary mining tradition, develops megaprojects at an altitude of 2,000 to 5,000 m and one of the largest consumers of energy in this sector relies on the transport of mineral, which today is carried out by trucks that consume large volumes diesel. (approximately 1500 gallons / day).

Studies in China (Lei et al., 2010; Lei et al., 2011) used ethanol blends to replace diesel in percentages of 10, 15, 20 and 30% v / v in diesel engines operating at altitudes simulated up to 2000 m, in a laboratory located 100 m high. Their results show slight increases in HC and CO emissions, without showing changes in NOx emissions. Likewise, research carried out with mixtures of diesel and ethanol with an oxygenation level of 2, 2.5 and 3.2% (Liu et al., 2014) on particulate matter and specific fuel consumption show that particulate matter emissions and specific consumption of Fuel is reduced with the use of ethanol in diesel, the most notable reduction being at altitude conditions.
These results motivate further development of tests under other experimental conditions limited to the high Andean region. In this work, the effects of diesel-biodiesel-ethanol mixtures are investigated in a diesel engine that operates at different pressures of the intake air at the compressor inlet, partially simulating operation at altitude.

1.1 Objectives

Define three stable diesel-biodiesel-ethanol blends and estimate their main physical-chemical properties.
Implement instrumentation and testing protocol for a Diesel engine using diesel-biodiesel-ethanol blends.
Evaluate the effects of combustion, specific fuel consumption and emissions of the exhaust gases of the engine under study.

Simulate partial operation of the engine at altitude and evaluate its effects on the engine performance.

2. Literature Review

Around the word the effects of diesel-biodiesel-ethanol mixtures are studied by researchers. They try to find alternative fuels to protect the environment and maintain the engine performance. Solis et al. (2016) conducted tests to determine the effective power, torque, consumption specific fuel and yield index in an agricultural engine using diesel fuels B5 and their mixtures with anhydrous ethanol (E) under the following percentages: 3% (ED3), 6% (ED6), 9% (ED9), 12% (ED12) and 15% (ED15). From this, they observed that the maximum power was obtained for fuels ED3, B5 and ED6 with maximum values of 76.07, 75.92 and 75.46 kW respectively. On the other hand, the mixtures ED9, ED12 and ED15 presented reductions in the maximum effective power of 3.32, 3.74 and 7.53% respectively. However, the authors do not substantiate the drop in engine power. By On the other hand, with respect to torque, the measured values for B5 and ED3 do not differ much; in contrast, the mixture ED12 and ED15 presented reductions of 2.91% (10.8 N.m) and 6.29% (23.36 Nm) compared to diesel B5. These reductions were explained by the increase in the number of cetane and low calorific value of ethanol. For specific consumption fuel, it was observed that this decreased as the concentration increased of ethanol in the mixture with the exception of ED3, which did not show a substantial change. The authors concluded that ethanol in diesel can be used without changing engine performance for ethanol values less than 12%. Sahin and Durgun (2016) conducted studies to determine the effects of ethanol (EF) on the diesel in performance parameters and NO_X emissions of an aspirated diesel engine natural. The ethanol was supplied via a carburetor in the engine's air intake, which adjusted the ethanol injection by a screw, in percentages of 2, 4, 6, 8, 10 and 12% of the volume approximately (EFO). In addition, the trial was conducted at delivery rates of 1 / 1FDR and 3 / 4FDR fuel (FDR) and six different speeds: 1500, 2000, 3000, 3500 and 4000 rpm (Sahin et al., 2016). Dugru and Bulut (2016) conducted experiments with ethanol-diesel and canola-diesel mixtures in a Diesel engine. The mixtures analyzed were in volumetric percentages of 5% (B5 and E5), 10% (B10 and E10) and 15% (B15 and E15) for both canola-diesel and ethanol-diesel blends. The tests were carried out to determine the parameters of torque, effective power, specific fuel consumption and effective efficiency for engine speeds between 1200 and 2400 rpm with intervals of 400 rpm. The results showed that the canola and diesel mixtures decreased the torque and the effective

power, which was most relevant at 2400 rpm. On the other hand, the mixture B5 and B15 decreased torque and effective power, both of which were most noticeable at 2400 rpm. By On the other hand, the mixture B5 and B10 provided a fuel economy of 1.3% in the ranges from 1500 to 1800 rpm; and B5 gained 2.2% effective efficiency compared to diesel fuel. Ethanol (96% purity) caused a decrease in horsepower and torque 25 the motor; For example, the E15 mixture decreased torque by 6.7% and effective power by 7.3%, on average. In addition, the E5 mixture increased the specific fuel consumption by 3.7% for ranges from 1600 to 2400 rpm and the E15 mix increased by 3% in efficiency.

effective compared to diesel. Costa et al. (2007) developed experimental tests to determine the influence of cetane number (CN) from 42 to 48 on emissions in two Euro III engines (engine with common rail injection system and Unit Pump System). For this they used three types of fuels additives with cetane; maintaining, where possible, the density and content sulfur. Through an analysis of variance and correlation techniques, the results did not show Significant NC trends on polluting emissions and fuel consumption. The researchers conclude that the increase in cetane from 42 to 48 CN in EURO engines III does not influence the emissions of CO, HC, NOx and CO_2, nor the specific consumption of fuel. Tutak et al. (2017) developed experimental tests varying the diesel-ethanol mixtures and biodiesel -ethanol from 0 to 45%, with an increase in ethanol of 5% over diesel or biodiesel. The tests were performed on a naturally aspirated, single cylinder, direct injection MEC and constant rotation speed of 1500 rpm. The researchers found that the mixture Diesel-ethanol presented its highest thermal efficiency for a mixture of 35% ethanol on the diesel. The exhaust gases had a higher temperature for the diesel-ethanol mixtures than for biodiesel ethanol. The maximum NO_X emissions were for the mixtures of 35 and 45% of ethanol over diesel and biodiesel with values of 5.5 and 3.5 g / kWh respectively. The CO emissions decrease with the presence of ethanol; emissions reach values of 2 and 1.5% for diesel-only and biodiesel uses respectively; for a substitution of 26 45% of ethanol in the mixture, CO emissions were reduced by up to 0.4% for both the diesel as well as biodiesel. Finally, CO_2 emissions had to increase with the ethanol content; for a 45% substitution of ethanol over diesel and biodiesel, the CO_2 emissions increased 8 and 7% respectively. Abhishek et al. (2017) developed a complete analysis of combustion in an MEC of 4 times, 1 cylinder, naturally aspirated and direct injection. Diesel blends were used and ethanol with a type of biodiesel (pongamia piñate methyl ester, PPME) as a co-solvent for avoids phase separation; the HIPC concentration was 50%. Ethanol concentration it was varied from 0 to 20%, in 5% intervals. The analysis of performance, exergy, combustion and emissions analysis (compared to the 100% diesel blend) led to the conclusion that the mixture D35E15B50 with 15% ethanol presented the best thermal efficiency with a increase of up to 21.17% and a decrease in with specific fuel consumption of up to 4.61% at full load; the same mixture showed a decrease in hydrocarbons not burned, but an increase in NO_X emissions. Also, the fuel D35E15B50 presented an increase in exergetic efficiency of 22.02% and a decrease of exergetic destruction of 21.06%. Tongroon et al. (2019) evaluated diesel-ethanol mixtures (also called diesol) together with a co-solvent (biodiesel) to avoid phase separation, obtaining the following mixtures: B3E5, B7E5 and B10E10. In this investigation, a 4-stroke, 4-cylinder and 4-cylinder MEC was used. direct injection. The pilot fuel injection was delayed due to the longer ethanol evaporation. HC emissions were increased by the longer time of delay of combustion; and NO_X emissions increased due to increased heat release during the premixed combustion phase. 27 Wei et al. (2018) investigated the effects of biodiesel-ethanol and biodiesel-butanol mixtures on a naturally aspirated, four-cylinder direct injection Diesel engine. The experiments were conducted with mixtures BE5 (5% ethanol and 95% biodiesel), BE10, BE15 , BBu10, BBu15 and 6 load factors at 1800 rpm. They analyzed the characteristics of the combustion, the effects on the rate of heat release, the maximum pressure increase combustion, specific fuel consumption, thermal efficiency and emissions pollutants. The results show that the mixtures of BE and BBu show an increase in the delay of combustion and a greater release of heat during the premixed phase; likewise, they presented an increase in specific fuel consumption and a slight influence on thermal efficiency. On the issue of emissions, the BBu mix presented a increase in CO emissions of 13.7% and HC of 5.6%; and the BE mix featured a increase in CO emissions of 22.8% and HC of 29.2%. However, the emissions of NO_X presented a decrease of 6.5% for BBu and 28% for BE. From these results, the researchers conclude that BE mixtures are more effective in reducing particulate matter and NO_X and BBu mixtures have a lower increase in emissions of CO and HC. Shamun et al (2018) conducted research on Diesel blends, biodiesel and ethanol in volumetric ratios of 68:17:15 and 58:14:30 respectively on a Supercharged mono cylindrical MEC, with intercooler and direct injection. Parameters studied were linked to engine performance and polluting emissions. The Results found that fuels with incorporated ethanol present an efficiency of 52%; On the other hand, fuels with only diesel have an efficiency of about 48%. NO_X and particulate matter emissions were reduced with the presence of ethanol; however, at low loads, HC and CO emissions were very high for mixtures with associated ethanol. Shahir et al. (2018) conducted a bibliographic review of various authors on the effects of the mixture of diesel, biodiesel and ethanol on MEC engines. The results of various Scientists and researchers presented that the properties of mixtures with ethanol are similar to diesel fuel. Likewise, mixtures with

ethanol reduce emissions of particulate matter. However, the emissions of NO_X, CO_2, CO and HC depend on the engine operating conditions. Lei et al. (2011) investigated the effects of diesel-ethanol mixtures on different regions altitude in China. The experiments were developed on a 4-cylinder MEC engine, supercharged and direct injection operating with blends E10, E15, E20 and E30 and at different atmospheric pressures (81 kPa, 90 kPa and 100 kPa). The experiments presented that specific fuel consumption increases as pressure decreases atmospheric. HC and CO emissions increase with increasing angular velocity, engine charge and ethanol in fuel. Changes in atmospheric pressure have no effect on NO_X emissions. Emissions of particulate matter decrease with the increase of ethanol and with greater incidence at atmospheric pressures lower than 90 kPa. He et al. (2014) conducted experiments on an MEC with intercooler, supercharged, 6 cylinders and direct injection. In order to assess the effects of altitude on emissions pollutants, a test bench was simulated for two altitude levels (1000 and 2000 masl). The experimental results indicated that at high altitudes (2000 masl) the emissions of HC, CO and particulate matter increase by values of 30%, 35% and 34%. Emissions of NO_X varied according to engine conditions. At 2000 meters above sea level, the particulate matter is between 1.6 and 4.2 times higher than at 1000 meters over the sea (He et al., 2011). Liu et al. (2014) developed research on diesel, biodiesel and ethanol blends simulating various atmospheric pressures (100, 90 and 81 kPa). Oxygenated mixtures with 29% ethanol had an oxygen concentration of 2%, 2.5% and 3.2% by mass. The results indicated that oxygenated fuels reduce engine torque. in the messure that reduces the atmospheric pressure, the specific fuel consumption decreases, as well as the Oxygenated fuels do not have any influence on the specific consumption of fuel. Emissions of particulate matter decreased at lower pressures atmospheric conditions and with the increase of oxygenated fuels. Ji-Lim et al. (2011) investigated the effects of diesel-ethanol blends under different altitude regions in an intercooled, supercharged, 4 cylinder MEC and direct injection. The mixtures varying the percentage of ethanol were E10, E15, E20 and E30 at atmospheric pressures of 81, 90 and 100 kPa. The results at 81 kPa showed that the HC and CO emissions increase with crankshaft speed, engine load and increase of ethanol in the mixture. While at 90 and 100 kPa the increase in emissions of HC and CO are very light with the increase of the speed in the crankshaft, load of the engine and ethanol supplemented to the mixture. On the other hand, changes in atmospheric pressure and the effects of ethanol in the mix have no effect on NO_X emissions. The bibliographic review, preceded in this chapter, makes it possible to identify the opportunities and prospects for the use of biodiesel and ethanol fuels in existing diesel engines nowadays. In addition, the research altitude effect research over the engines is important.

3. Methods

The study was carried out on a diesel engine, 6 cylinders, four times, with supercharging and intercooler; common rail injection; 6.7 l; 119 kW @ 2200 rpm; Cummins QSB6.7. The motor was coupled by means of a cardan shaft to a water-cooled electric dynamometer. The values of torque, speed of rotation and temperatures of the engine cooling system and dynamometer were regulated by means of a control module. The experimental scheme of the test bench is presented in Figure 1.

Different temperature, pressure, flow, relative humidity and pollutant concentration sensors were used to monitor engine fluid conditions. The temperatures of the air, refrigerant and lubricant were measured by means of platinum resistance thermometers (PT100), while the measurements of the temperature of exhaust gas were measured with thermocouples type k. The pressures were recorded through piezoresitive transducers classified in the range of 0 to 250 bar (uncertainty ± 0.3% FS) and - 1 to 2 bar (uncertainty ± 0.004%).

The air flow was measured by a laminar flow device, Meriam brand, model 50MC2-6 (uncertainty ± 1% for the range of 0 to 2500 Pa of the pressure differential). Fuel consumption was measured by flow meter type coriolysis, Emerzon brand model CMF010M (uncertainty of ± 0.05%). Relative humidity and ambient air temperature, in the test room, was measured with a microphone type sensor, Omega brand, model HX94 (uncertainty ± 2% RH / ± 0.6 ° C, range from 3 to 90% RH / 0 to 100 ° C). Data from these sensors was collected by a Honeywell brand electronic data logger using a 1Hz sampling rate.

For the study of combustion, a pressure transducer of the piezoelectric type was used, together with a piezoresitive transducer, optical encoder, current clamp, signal amplifier and AVL Puma Open acquisition system. The piezoelectric sensor model GU21D (uncertainty ± 0.3% FS, range 0-250 bar) was used to measure the pressure inside the first cylinder of the engine. The Model XXYY piezoresistive sensor was installed in the engine air manifold, close to the first cylinder intake valves. This sensor allowed correcting the piezoelectric sensor signal for absolute pressure conditions. The measurement of the angle of rotation of the crankshaft of the engine was collected by means of a model 365C encoder; The information obtained by means of light pulses from the encoder was transferred by an optical cable to an optical transducer and a pulse multiplier, allowing a resolution of 0.5 crank angle deegre (CAD).

To determine the coil energization time (SOE) corresponding to the first fuel injector, a current clamp model TI0602ACCA was used. All these electrical signals from the AVL components were processed through an AVL Indimicro interface.

The concentrations of NO_X, CO and CO_2 in the engine exhaust gas were sensed by a Testo brand portable gas analyzer, model 350-XL.

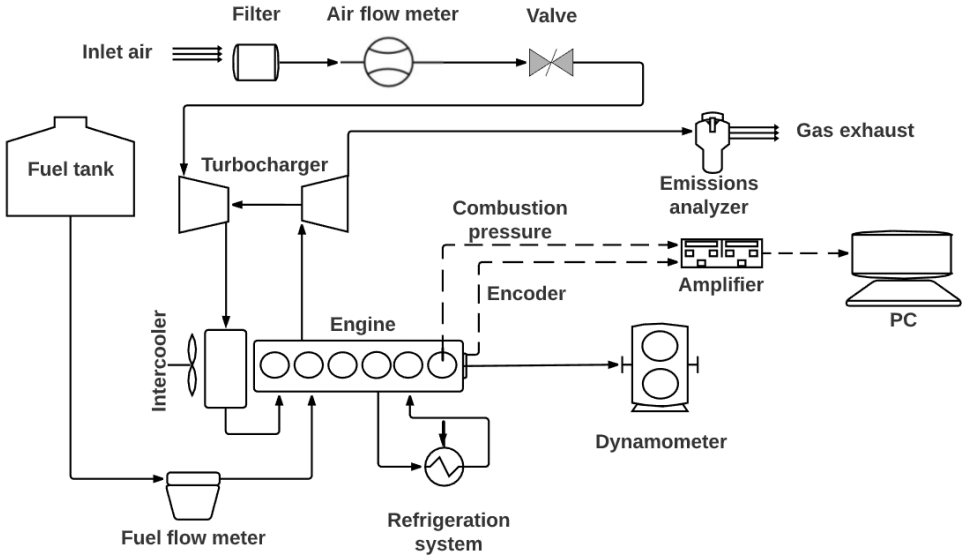

Figure 1. Experimental configuration

4. Data Collection

In the present study, the effects of anhydrous ethanol (E) and biodiesel (B) mixed with Diesel fuel (D), which originally contained 5% biodiesel by volume, were analyzed. Castor oil was used to increase the total amount of biodiesel in the mixture, furthermore it compensates for the low lubricity and stability due to the use of ethanol (Hansel et al., 2005; Gagliuffi, 2000).

In total, three fuel mixtures were used, differentiated by the volumetric content of ethanol from 0% (E0) to 13.5% (E13.5): D95B5E0, D85B6E9 and D80B6.5E13.5. The estimated physicochemical properties of fuels are presented in Table 1. These properties were determined using the correlations of Clement and Modified Lederer (Muralee et al., 2019; Saxena et al., 2013).

Table 1. Propiedades físico-químicas de las mezclas combustibles.

Property	Commercial diesel	Commercial ethanol	Castor oil	D95B5E0	D85B6E9	D80B6.5E13.5
Density, kg/m^3	840	786	926	840	836	834
Cetane number	45.0	8.0	38.0	45.0	41.6	39.9
Low heat value (LHV), MJ/kg	42.5	28.4	37.5	42.5	41.2	40.5
Kinematic viscosity at 40°C, cSt	4.10	1.40	14.10	4.10	4.02	3.98

The experimental tests were carried out under stationary conditions, setting a speed and a certain torque of the motor. The experiment matrix was defined by two rotational speeds (1000 and 1800 rpm), two levels of effective torque (80 and 160) and two intake air pressures (100 and 80 kPa) measured at the turbocharger inlet (AICP) . The control of the

AICP pressure allowed to simulate, in part, the behavior of the engine at two levels of altitude. In total, 18 test points were obtained, each of which was defined by a torque, a rotation regime and an AICP value.

Initially, the experimental procedure consisted of verifying the correct operating conditions of the engine, dynamometer and instrumentation used. Then, the engine was preheated until the proper working fluid temperatures were reached (80 ° C and 110 ° C for the coolant and lubricating oil, respectively). Once the initial condition was established, the torque and rotation of the engine were adjusted through the dynamometer control and, likewise, an AICP value was adjusted by means of a butterfly valve installed in the engine intake. Once the operating conditions were defined at a test point, it was waited for a period of two minutes until a stable engine condition was reached and data acquisition began.

The data from the sensors installed on the test bench were recorded for three minutes, at a sampling frequency of 1 Hz; while the sensors linked to the study of combustion recorded 100 thermodynamic cycles, with sampling frequencies of up to 43 kHz.

4.1 Start of combustion

In this investigation, the criterion of the second derivative was used by means of the pressure signal inside the cylinder as a function of the crankshaft angle of rotation to determine the start of combustion, SOC; This criterion analyzes the change in concavity of the dp⁄dθ signal (Sahin and Durgun, 2016; Assanis, et al., 2003). The SOC corresponds to the minimum value of the first derivative of dp⁄dθ, that is, when $d^2p/d\theta^2 = 0$.

4.2 Maximum rate of pressure rise during combustion

Once combustion has started, the pressure inside the cylinder increases suddenly until it reaches a maximum pressure, MPRR (equation 1). The instantaneous increase in pressure is related to the high speed of energy release during the pre-mixed combustion phase (Heywood, 2018). However, high rates of energy release can reduce the life of the piston, valves, cylinder head, and increase engine vibration and noise (Lowe et al., 2011).

$$\boldsymbol{MPRR = (dp/d\theta)_{máx}} \tag{1}$$

4.3 Rate of heat released during combustion

The net rate of heat released, NHRR, allows analyzing the progress of the combustion process, once the oxidation of the fuel has started. For this, the thermodynamic model of a zone is used, which is based on the first law of thermodynamics for an open system (the contents of the cylinder) considering quasi-static conditions, that is, pressure and uniform temperature (Heywood, 2018; Kumar, 2019). The net rate represents the difference between the gross rate of the heat released and the rate of heat transfer to the walls, which is equal to the rate of work done on the piston plus the rate of change of the sensible energy, of the contents of the cylinder. Additionally, it is assumed that the cylinder contents can be modeled as an ideal gas, obtaining equation (2).

$$\mathbf{NHRR} = \frac{\boldsymbol{\gamma}}{\boldsymbol{\gamma - 1}}\mathbf{p}\frac{\mathbf{dV}}{\mathbf{d\theta}} + \frac{\boldsymbol{\gamma}}{\mathbf{1 - \gamma}}\mathbf{V}\frac{\mathbf{dp}}{\mathbf{d\theta}} \tag{2}$$

On the other hand, since the rate of heat released is a function of the first derivative of the cylinder pressure, its fluctuations are magnified on the NHRR representation. This leads to inaccurate detection of the onset of heat release. Therefore, the Fourier transform is applied to filter the high-frequency portion of the data from the released heat and eliminate noise, which is typically over 〖10〗 ^ 4 Hz, preserving the physical characteristics of the signal (Cuisano et al. ., 2019; Flores, 2019). The rate of heat released is later reconstructed with the inverse Fourier function according to equation (3).

$$\mathbf{NHRR} = \mathbf{NHRR_{avg}} + \sum_{\mathbf{n=1}}^{\mathbf{N}} [\mathbf{A_n cos(n\theta) + B_n sin(n\theta)}] \tag{3}$$

$NHRR_{avg}$ is the average net rate of heat released, A_n and B_n are the Fourier coefficient, θ = ωt, where ω is the angular frequency and t is the time, n is the harmonic number.
Here it is important to mention that the SOC, described above, was also obtained from the NHRR curve, because this parameter includes the dp⁄dθ signal in its formulation.

4.4 Specific fuel consumption

One way to evaluate the performance of an internal combustion engine is through fuel consumption, $\dot{m}_f$. However, due to the differences that occur depending on the power developed, it is convenient to use the term specific fuel consumption (sfc), in g / kWh, which is determined and defined as the relationship between the mass consumption of fuel and the effective power P of the motor. Equation (4) represents the sfc.

$$\mathbf{sfc} = \frac{\dot{\mathbf{m}}_\mathbf{f}}{\mathbf{P}} \tag{4}$$

4.5 Specific emissions

Exhaust emissions are products of combustion between the fuel and the mass of air supplied to the engine within the combustion chamber. These emissions come out through the exhaust pipe and are measured by means of an analyzer. Emission levels can be expressed in different ways, which can sometimes lead to difficult and ambiguous comparisons. Therefore, in Diesel engines, it is common to express emissions in specific terms, EE in g / kW.h, dividing the mass flow of the pollutant by the effective power developed by the engine.

Equation (5) was used to determine the specific emissions of nitrogen oxidesEE_{NO_X}, carbon monoxide EE_{CO}O and carbon dioxide EE_{CO_2} (Hernandez et al., 2015; Gautam, 2001). In this expression, $\dot{m}_{air}$ is the mass flow of the intake air to the engine, M_x is the molecular weight of the pollutant x, X its volumetric fraction.

$$EE_x = \frac{\dot{m}_f + \dot{m}_{air}}{P}(M_x . X) \tag{5}$$

5. Results and Discussion

5.1 Combustion characteristics

Figures 2 to 4 show the results of the parameters related to the combustion process using three fuel mixtures (D95B5E0, D85B6E9 and D80B6.5E13.5) and two simulated altitude conditions (APCI of 100 and 80 kPa), for 12 points of test (2 rotational speeds, 1000 and 1800 rpm; 2 effective torques, 80 and 160 Nm).

In Figure 2, the pressure curves within the cylinder and the net rate of heat released are presented. With the restriction of the air in the intake (from 100 to 80 kPa) that partially simulates the effect of the operation at altitude, lower levels of pressure were generated inside the cylinder; but no appreciable effect on the NHRR curves. The NHRR curves show the two combustion phases in the Diesel engine, pre-mixed and diffusive. The higher the torque, the m˙_f increases, helping the second phase of combustion (diffusive) to appear more accentuated.

At 1000 rpm, SOC occurs before TDC, between -10 and 0 CAD; while at 1800 rpm, combustion starts after TDC, between 0 and 10 cad. Likewise, at 1000 rpm, a greater effect of the biodiesel mixture with ethanol is observed on the evolution of the pressure and NHRR curves. At lower torque (80 Nm) and regardless of the adjusted APCI, the use of the D85B6E9 causes greater advances in SOC. Similarly, in general, the effects of the mixture of biodiesel and ethanol tend to present less intensity of the pre-mixed combustion (first phase of the heat released); this due to the advancement of the SOC. The slight advance of the SOC would be linked, in part, to the better atomization of the mixture containing a higher percentage of ethanol, causing a lower viscosity in the mixture (Table 1).

At 1800 rpm, small variations in filtered pressure cause certain fluctuations in the heat released rate curves. But, in general, there is a slight increase in the SOC lag with the use of D85B6E9 and D80B6.5E13.5, compared to commercial fuel. This effect would be associated with the effect of the lower cetane index (Table 1) with the higher fuel demand during the higher rotation regime. Another aspect noted is that, regardless of the fuel used in the tests, it is found that the lower APCI value (80 kPa) reduces the intensity of the pre-mixed combustion and increases the intensity of the diffusive combustion. However, the greatest peaks of diffusive combustion occur with the use of mixtures containing a greater volume of oxygenated fuels.

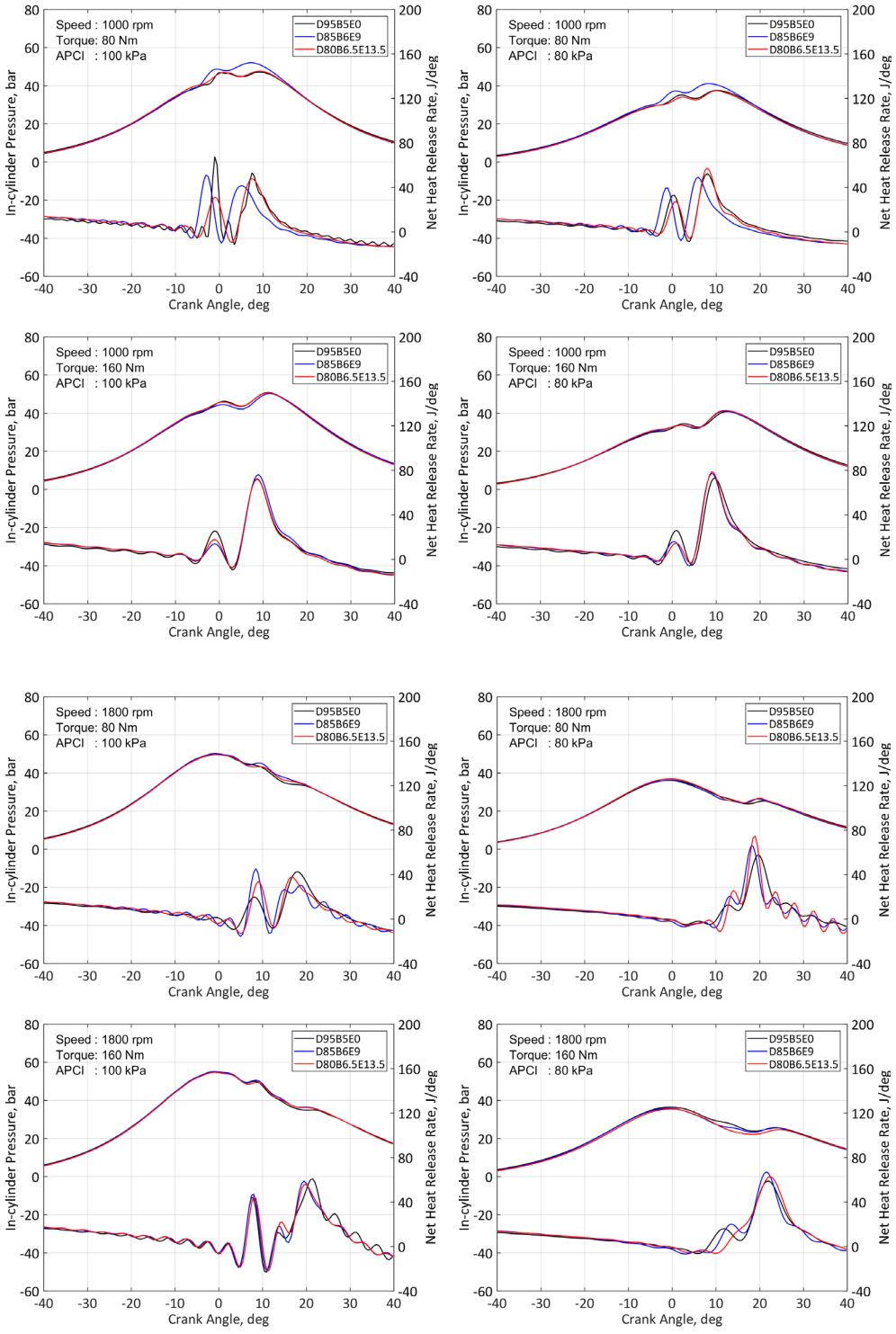

Figure 2. Pressure and net heat release rate traces for diverse fuel blends at different load and absolute pressure at the compressor inlet (speed: 1000 and 1800 rpm).

Figure 3 presents the results of the maximum pressure rise rate (MPRR) during the combustion process of the first cylinder of the engine. The MPRR values are greater than 1000 rpm, before TDC, varying from 1.64 to 3.67 bar / deg;

while at 1800 rpm, the MPRR occurs after TDC, reaching values that vary from 1.18 to 1.79 bar / deg. The lower gradient at 1800 rpm, in the expansion stroke, is affected by the higher piston speed.
With the higher percentage of ethanol in the fuel mix, there is generally a bias towards a small increase in MPRR relative to the use of commercial fuel. Such an effect, however, is more outstanding during operation at higher torque (160 Nm at 1000 rpm) and using D80B6.5E13.5. Restricting the APCI, from 100 to 80 kPa, does not alter the general trend of the MPRR; and at 80 N.m, there is no defined orientation of the MPRR. These results can also be inferred from the slopes in the NHRR curves during the diffusive or premixed combustion phases (Figure 3).

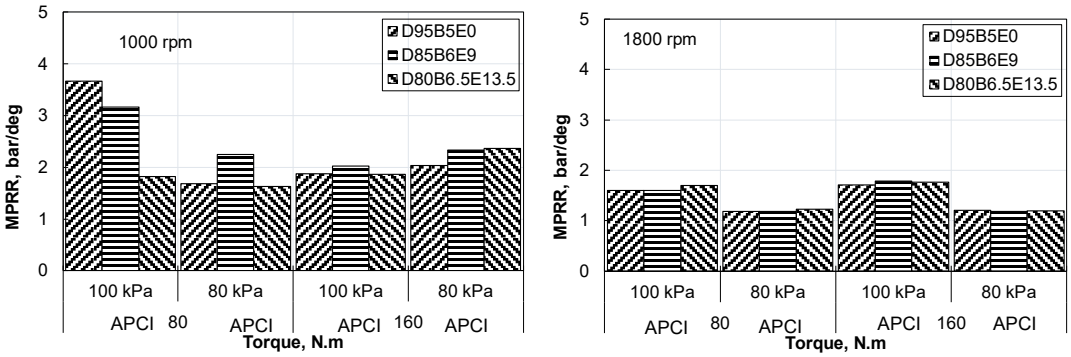

Figure 3: Maximum rate of pressure rise during combustion in the first cylinder of the engine

Figure 4 presents the maximum pressure during combustion (MCP) in the first cylinder of the engine. The MCP is the result of the change from heat energy to mechanical energy translated into pressure on the surface of the piston. Likewise, when combustion occurs after TDC, as it occurs at 1800 rpm, generates an MCP, which is associated with the effective power in the shaft and the amount of heat released during the pre-mixed and diffusive combustion phase (Heywood, 2018). In general, the MCP values do not show a clear trend due to the effect of fuel. But there was a decrease in MPC for the tests with APCI at 80 kPa compared to 100 kPa for APCI, reducing the pressure to 34.5% at 1800 RPM and 160 N.m.

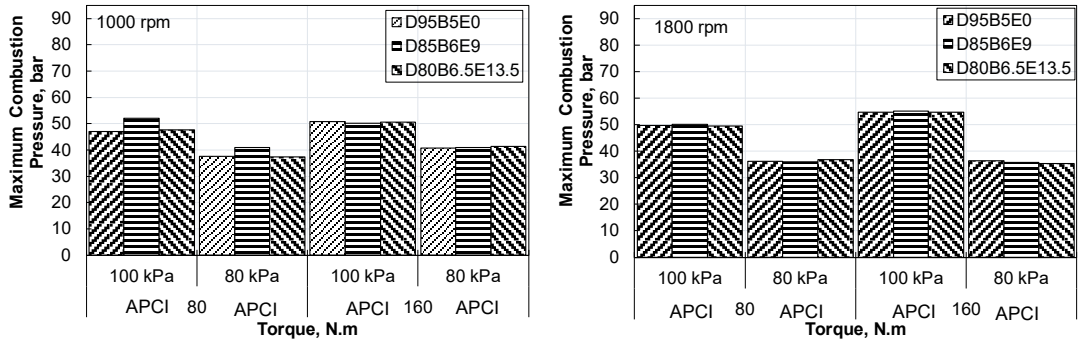

Figure 4. Maximum pressure during combustion in the first cylinder of the engine

5.2 Specific fuel consumption

Figure 5 presents the specific fuel consumption (sfc). This is a very useful parameter to determine the efficiency of the motor (Payri, 2011). As expected, the tests at 1000 and 1800 rpm show higher sfc at low torques, since the mechanical losses are more significant with respect to the useful power of the engine (Heywood, 2018).

Regarding the use of different fuels, it is noted that, in general, there is a slight increase (up to 9%) in the sfc value with the highest ethanol content in the mixture. This effect is associated with the lower calorific value when using a higher percentage of biofuels (Table 1). At low torque, the D85B6E9 and D80B6.5E13.5 blends decrease the engine sfc relative to its operation with commercial fuel. Such is the case of the test point at 80 N.m and 1800rpm, where the sfc decreases by 13% with the use of D85B6E9 compared to D95B5E0.

Also, during simulated altitude tests, in general, there is an increase in sfc of up to 11% for the D95B5E0 fuel, due to the fall of the APCI; therefore, lower pressure and initial working temperature in the combustion chamber.

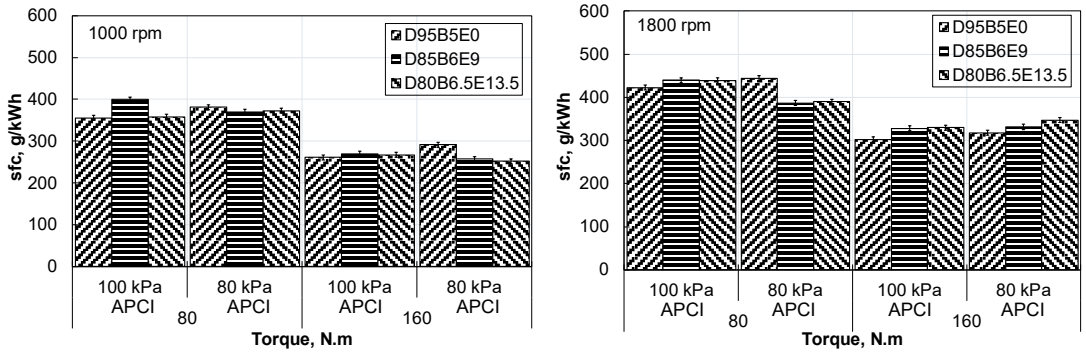

Figure 5. Specific fuel consumption at the different engine test points

5.3 Characteristics of specific emissions

In general, higher specific emissions are associated with higher values of sfc, due to the fact that when a greater mass of fuel is injected, there is a greater quantity of polluting products originated during the combustion process (Heywood, 2018). This is corroborated when comparing the results of EE of CO_2 (Figure 6), CO (Figure 7) and NO_X (Figure 8) versus sfc (Figure 5).

The CO_2 EEs at 1000 and 1800 rpm, with different load and APCI settings, ranged from 727 to 1418 g / kWh, with uncertainties between ± 6.3 and ± 14.7 g / kWh. At 1000 rpm, Figure 6 clearly shows that the highest CO_2 EEs correspond to the commercial fuel D95B5E0, and as the use of ethanol and biodiesel in the fuel mix increases, these emissions tend to decrease. Similar effects occur during simulated altitude operation. At the operating point at 80 Nm, 1000 rpm and 100 kPa, CO_2 EEs decrease by 25 and 30% with the use of D85B6E9 and D80B6.5E13.5, respectively. Similar results were reported in other studies (Shair et al., 2015; Tutak et al., 2017) indicating that this effect is due to the lower carbon content in oxygenated fuels, which causes lower CO_2 emissions and more H_2O. At 1800 rpm, EEs are generally very similar between the three types of fuels; With the exception of the operating point at 80 Nm and 100 kPa, any apparent difference in the CO_2 EEs between the three fuels is covered by the experimental uncertainties.

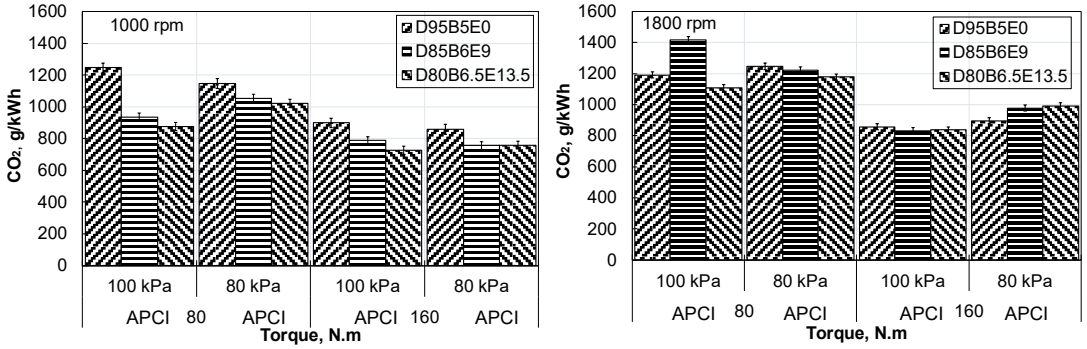

Figure 6. Specific CO_2 emissions

Figure 7 presents the EE of CO, varying from 2.8 to 12.3 g / kW.h, with experimental uncertainties between ± 0.1 and ± 0.3 g / kWh. These pollutants are produced during combustion, when the adiabatic flame temperature is reached (CO emissions are formed from 2000 K) and are products of an incomplete combustion of the oxidation process of CO to CO_2, which is very recurrent during the pre-mixed combustion phase and with the use of rich air-fuel mixtures (Payri et al., 2011).

Similar to CO_2 emissions, the CO results at 1000 rpm corroborate that the use of higher percentages of ethanol and biodiesel in the fuel mixture reduces these emissions by up to 29% when using D80B6.5E13.5, with respect to the EE

generated with commercial fuel. Once again, the explanation lies in the presence of the OH radical in oxygenated fuels; Add to this the use of poor air-fuel mixtures and high evaporation temperature of ethanol, which generate lower temperatures inside the cylinder, resulting in a reduction of the EE of CO.

At 1800 rpm, the CO EEs show an increase when using fuels added with ethanol and biodiesel. This effect is associated with the higher fuel intake and the less lean dosing of the air-fuel mixture that causes a lack of oxygen inside the combustion chamber. Likewise, the higher the regime (shorter time for the oxidation of the fuel), the fuels added with ethanol cause a greater delay in the start of combustion (Figure 2), contributing to the higher EE of CO in the exhaust gas.

However, other research shows an increase in CO emissions at low rpm and a decrease at high rpm, arguing the high evaporation temperature of ethanol, which is more considerable at high temperatures (Lei et al., 2010). This argument can be disagreeable, since at high rpm the pressure inside the cylinder is higher, which increases the temperature inside the combustion chamber and thus favors the formation of CO emissions.

On the other hand, during simulated altitude tests, CO emissions increased, regardless of the fuel used, which is correlated with other studies due to the increase in sfc (he et al., 2011). But at 1800 rpm this is further emphasized with the use of the D85B6E9 and D80B6.5E13.5. Such is the case at 160 N.m, where the CO EEs with the D95B5E0 increased from 3.7 to 6.1 g / kW.h by restricting the APCI from 100 to 80 kPa. This difference represents an increase of 64%. And if the D80B6.5E13.5 (8.4 g / kWh) is used in 80 kPa of APCI, the EE of CO would increase by 128% compared to the operation with D95B5E0 and 100 kPa.

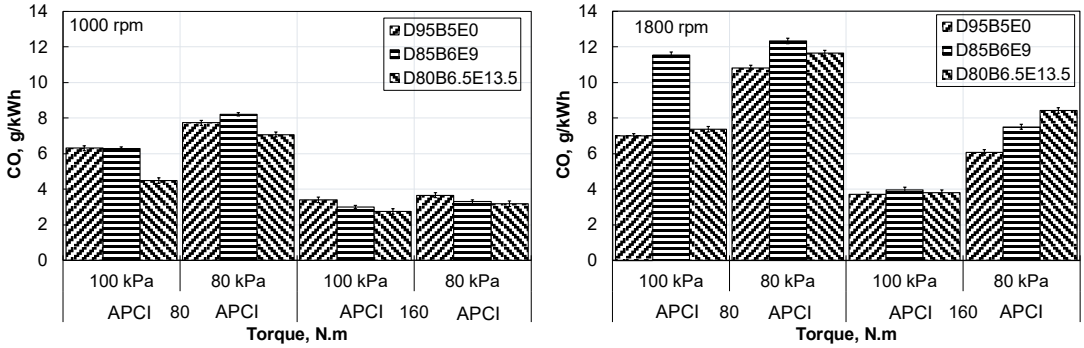

Figure 7. Specific CO emissions

The EE of NOx are shown in Figure 8. The EE of NO_X corresponds to the sum of the emissions of NO_2 and NO, which has a greater presence of NO because they are generated at high temperatures (more than 2000 K); Instead, NO_2 results from the conversion of NO at low temperatures (less than 1800 K) and high presence of oxygen (O2) (Payri et al, 2011).

In Figure 8, the EE of NO_X vary from 1.6 to 6.7 g / kW.h, with experimental uncertainties between ± 0.1 and ± 0.2 g/ kWh. At 1000 rpm, the EE of NO_X show a tendency to decrease as the content of ethanol and biodiesel increases, to a lesser extent, in the fuel mixture; being the mixture D80B6.5E13.5 the one with the lowest NO_X emissions with a decrease of up to 26% (at 80 N.m and 100 kPa) compared to the commercial fuel D95B5E0. This effect is related to the previous results of the NHRR (Figure 2), where a lower intensity of the pre-mixed flame was verified with the greater use of biofuels. The higher ethanol content requires more energy to vaporize, resulting in a lower flame temperature.

Also, at 1800 rpm, the behavior of the NHRR premixed phase is related to the trend of NO_X EE. At 80 Nm, with and without intake air restriction, it is verified that the higher intensity of the pre-mixed combustion with the D85B6E9 and D80B6.5E13.5 are responsible for the slight increase in their respective NO_X EE. At 160 Nm, biofuels do not affect NO_X EE.

Operations simulating altitude, at 1000 rpm, cause higher CO emissions (Figure 7) and lower NO_X EE (Figure 8). However, at 1800 rpm, this exchange does not stand out. Likewise, NO_X emissions vary with the type of engine and working conditions (He et al., 2011).

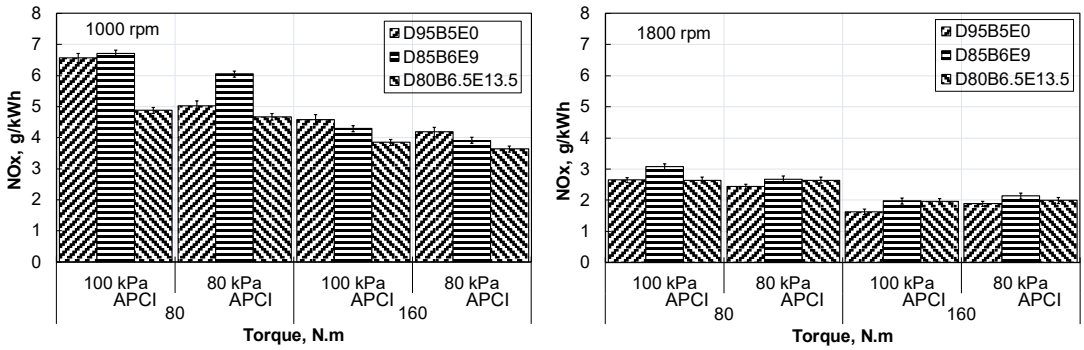

Figure 8. Specific NO_X emissions

5.4 Validation

The global uncertainty of each parameter analyzed is associated with the quality of the measured data and the calibrated instruments used in this study. This uncertainty is quantitatively characterized by the standard deviation of the values obtained according to GUM (BIPM, 2008). The experimental works always present errors, which cause that there is a certain veracity in the values measured experimentally.

According to the GUM, the uncertainty of the result can be decomposed into several parameters that are composed of a certain degree of error. The uncertainty analysis is based on its main error propagation equation (see equation 6); where the global uncertainty ΔU, corresponding to the global parameter F(x), is estimated by the parameters $\mathbf{x_1}, \mathbf{x_2}, .., \mathbf{x_n}$, which have their own uncertainties $\mathbf{\Delta U_{x_1}}, \mathbf{\Delta U_{x_2}}, .., \mathbf{\Delta U_{x_n}}$. These considerations were taken for the analysis of the parameters that link to the data collected by the sensors of the test bench. Likewise, when necessary, the statistical criterion for data discernment proposed by Chauvenet (Milosa, 2017) was used.

$$\Delta U = \sqrt{\sum_{i=1}^{n} \left(\frac{\partial F}{\partial x_i} \Delta U_{x_i} \right)^2} \tag{6}$$

6. Conclusion

Specific fuel consumption, net rate of heat released, and exhaust gas emissions were analyzed in a 6-liter compression-ignition engine, operating at different simulated altitude conditions and using different blends of diesel, biodiesel, and ethanol. The commercial fuel is D95B5E0 and the alternative blends (D85B6E9 and D80B6.5E13.5) included volumetric percentages of up to 13.5% ethanol and, to a lesser extent, biodiesel.

The specific fuel consumption of the engine is not affected by the use of ethanol and biodiesel, despite the lower calorific value of the alternative blends. The results of the net rate of heat released show that the mixtures D85B6E9 and D80B6.5E13.5 slightly advance the start of combustion by 1000 rpm, with less intensity of the pre-mixed combustion phase. The opposite effect could be noticed at 1800 rpm, where a small delay in the start of combustion may occur due to the lower cetane number of the alternative mixtures; in addition, there is a greater intensity of the pre-mixed combustion.

The specific emissions of NO_X, CO and CO_2 increase with the higher sfc. The CO_2 EE decrease with the increase of ethanol and biodiesel in the fuel, because the OH radical of the oxygenated component would lead to a higher production of H_2O. At 1000 rpm, CO emissions are related to observed trends in CO_2; however, at 1800 rpm, CO EEs are increased with increased use of ethanol and biodiesel. These results are associated with the temperature levels

inside the combustion chamber (from low to high, as the engine speed increases). Oxygenated fuels decrease NO_X EEs during engine operation at 1000 rpm; but at 1800 rpm this contaminant is slightly increased by up to 21%.
On the other hand, the simulated altitude allowed to verify that at higher altitudes there is a slight increase in sfc and EE of CO and CO_2, together with a reduction in EE NO_X. At 2000 m of simulated altitude (APCI = 80 kPa) the maximum increases of sfc, CO and CO_2, with the mixture D80B6.5E13.5, were 5%, 122% and 18%, respectively. And the maximum reductions in NO_X EE were also obtained with the D80B6.5E13.5 mixture, reaching decreases of up to 6%.

References

Abhishek, P., Rajsekhar, P., Durbadal, D., "An Experimental study of Combustion, Performance, Exergy and Emission characteristics of a CI engine fueled by Diesel-Ethanol-Biodiesel Blends", doi: https://doi.org/10.1016/j.energy.2017.09.137, Energy, 141, 839-852 (2017).

Assanis, D., Filipi, Z., Fiveland, S., & Syrimis, M., "A Predictive Ignition Delay Correlation Under Steady-State and Transient Operation of a Direct Injection Diesel Engine", doi: https://doi.org/10.1115/1.1563238. ASME Journal of Engineering for Gas Turbines and Power, 125,pp. 450–457 (2003).

Gagliuffi, E., Guilherme, J. y Formiga, C., "Misturas diesel-álcool-óleo de rícino como um combustível Alternativo para motores de ignição por compressão", Centro de Tecnologia, Departamento de Engenharia Mecânica (2000)

Gestión, (02 de Julio de 2019). Gestión. Obtenido de https://archivo.gestion.pe/noticia/311269/diesel-lideraria-avance-demanda-mundial-combustible?ref=gesr.

GPAE, "Reporte semestral de monitoreo del mercado eléctrico, Organismo Supervisor de la Inversión en Energía y Minas", 12-13, Lima, Perú (2017).

Hansen, A., Zhang, Q., & Lyne, P., "Ethanol diesel fuel blends" – a review, doi: https://doi.org/10.1016/j.biortech.2004.04.007, Bioresource Technology, 96, 277–285 (2005).

He et al., "Emission characteristics of a heavy-duty diésel engine at simulated high altitudes", doi: 10.1016/j.scitotenv.2011.01.029 (2011) Science of the Total Environment, 409(17), 3138-3143 (2011).

Heywood, J., "Internal Combustion Engine Fundamentals". 2a Ed., McGraw-Hill, New York, Estados Unidos (2018).

Jayakumar, C., Zheng, Z., Joshi, U., Bryzik, W., Henein, N., & Sattler, E., "Effect of inlet air temperature on auto-ignition of fuels with different cetane number and volatility", doi: https://doi.org/10.1115/ICEF2011-60141, ASME, ICEF2011-60141 (2012).

Ji-Lin, L., Ze-fei, T., Shao-hua, L., Yu-Hua, B. y Li-Zhong, S, "Emission Characteristics of Diesel Engine Fueled with Ethanol-diesel Blends in Different Altitude Regions", doi: 10.1109/ICDMA.2010.43, 2011, 417-421 (2011).

Kumar, R., "Reciprocating Engine Combustion Diagnostics In-Cylinder Pressure Measurement and Analysis", 1a Ed. Springer Nature Switzerland AG, Cham, Switzerland (2019).

Lowe, D., Tian, R., Weiliang, W., & Tan, A. (2011). "Diesel knock combustion and its detection using. J. Acoustic Emission", 29, 78-88 (2011).

Lei, J., Bi, Y. y Shen, L., "Performance and Emission Characteristics of Diesel Engine Fueled with Ethanol-Diesel Blends in Different Altitude Regions", doi:10.1155/2011/417421, Journal of Biomedicine and Biotechnology, 2011, 10 (2011)

Liu, S., Shen, L., Bi, Y. y Lei, J., "Effects of altitude and fuel oxygen content on the performance of a high pressure common rail diésel engine", doi: 10.1016/j.fuel.2013.10.007, 118, 243-249 (2014).

Milosan, I., "Application of the chauvenet criterion to detection of the aberrant data obtained in the industrial processes", doi: Https://Doi.Org/10.19062/2247-3173.2017.19.1.47, Scientific Research And Education In The Air Force , 389-393 (2017).

MINAM. (02 de Abril de 2018). Ministerio del Medio Ambiente. Obtenido de http://www.minam.gob.pe/notas-de-prensa/a-partir-del-1-de-abril-del-2018-entro-en-vigencia-las-normas-de-emisiones-vehiculares-euro-iv-tier-2-y-epa-2007/

Muralee, S., Salam, P., Tongroon, M. y Chollacoop, N., "Performance and emission assessment of optimally blended biodiesel-dieselethanol in diesel engine generator", doi: 10.1016/j.applthermaleng.2019.04.012, 155, 525-533 (2019)

Organismo Supervisor de la Inversión en Energía y Minería, (29 de Dieciembre de 2018). Obtenido de http://www.osinergmin.gob.pe/empresas/hidrocarburos/Paginas/SCOP-DOCS/scop_docs.htm.

Payri, F., y Desantes, J., "Motores de combustión interna alternativos"., EDITORIAL REVERTÉ,S.A., Valencia, Espeña (2011).

Saxena, P., Jawale, S. y Joshipura, M., "A review on prediction of properties of biodiesel and blends of biodiesel", Pocedia Engineering, 51, 395-402 (2013)

Shamun, S,. Belgiorno, G., Blasio, G., Beatrice, C., Tunér, M., Tunestål, P., "Performance and emissions of diesel-biodiesel-ethanol blends in a light duty compression ignition engine", doi: https://doi.org/10.1016/j.applthermaleng.2018.09.067, Applied Thermal Engineering, 145, 444-452 (2018).

Sahin, Z. y Durgun, O., "Improving of diesel combustion-pollution-fijel ecomony and Performance by ethanol fumigation", J. of Thermal Science and Technology, doi: 10.1016/j.enconman.2013.07.068, 76, 620-633 (2013)

Shahirn, S., Masjuki nn, H., Kalam, M., Imran, A., Ashraful, A., "Performance and emission assessment of diesel–biodiesel–ethanol/ bioethanol blend as a fuel in diesel engines: a review", doi: https://doi.org/10.1016/j.rser.2015.03.049, Renewable and Sustainable Energy Reviews, 48, 62-78 (2015).

Tongroon, M., Saisirirat, P., Suebwong, A., Aunchaisri, J., Kananont, M y Chollacoop, N., "Combustion and emission characteristics investigation of diesel-ethanolbiodiesel blended fuels in a compression-ignition engine and benefit analysis", doi: 10.1016/j.fuel.2019.115728, 255(2019).

Tutak, W., Jamrozik, A., Pyrc, M., Sobiepański, M., "A comparative study of co-combustion process of diesel-ethanol and biodiesel-ethanol blends in the direct injection diesel engine", doi: https://doi.org/10.1016/j.applthermaleng.2017.02.029, Applied Thermal Engineering, 117, 155-163 (2017).

Wei, L., Cheung , C., Ning, Z., "Effects of biodiesel-ethanol and biodiesel-butanol blends on the combustion, performance and emissions of a diesel engine", doi: https://doi.org/10.1016/j.energy.2018.05.049, Energy, 55, 957-970 (2018).

Biographies

Julio cuisano is a Principal Professor, Director of Mechanical Department at Pontificia Universidad Católica del Perú and Innovation Group in Energy and Environmental Researchers Coordinator. He earned B.S. in Fluid Mechanics Engineering from Universidad Nacional Mayor de San Marcos, Lima, Masters in Mechanical Mngineering from Pontificia Universidade Católica Do Rio De Janeiro and PhD in Mechanical Engineering from Pontificia Universidade Católica Do Rio De Janeiro. He has published journal and conference papers. Dr julio has completed research in PUC-Rio, IFP Energies Nouvelles, Cmt-Motrores Térmicos. Universidad Politécnica De Valencia and Laben-PUCP.

Solin puma is a Master candidate of Energy and Environmental Master at Pontificia Universidad Católica del Perú, researcher, teacher in Energy Laboratory at Pontificia Universidad Católica del Perú. He earned B.S. in Mechanical Engineering from Pontificia Universidad Católica del Perú.